Al-Azhar Bulletin of Science Vol. 31, No. 2, (December), 2020, pp. 31-46

SYNTHESIS AND CHARACTERIZATION OF (AAM-CO-AHPS)/MMT HYDROGEL COMPOSITES FOR THE EFFICIENT CAPTURE OF METHYLENE BLUE FROM AQUEOUS SOLUTION

Amin Mohamed Elkony[1], Ahmed Galal Ibrahim [1,*], Maher Hamed Abu El-Farah[2], Farag Abdel Hai[1]

1 *Department of Chemistry, Faculty of Science, (Boys), Al-Azhar University, Nasr City, Cairo, Egypt*

2 *Egyptian mineral resources authority (EMRA), Dokki, Giza, Egypt*

*Corresponding author: ahmed_polytech@azhar.edu.eg, ahmed_polytech@yahoo.com

ABSTRACT

In this study, Acrylamide-co-3-Allyloxy-2-hydroxy-1-propanesulfonic acid sodium salt/ montmorillonite [(AAm-co-AHPS)/MMT)] hydrogel composite was synthesis via in situ free-radical copolymerization. The swelling properties and adsorption efficiency of MB were studied. Effect of AHPS ratio on the properties of hydrogel composite was investigated at different AAm/AHPS molar ratio of 100/0, 95/5, 90/10, 85/15, and 80/20. The highest swelling ratio (49.71 g/g) was observed for the composite containing 15% AHPS. The hydrogel composites were characterized using FTIR, TGA, XRD, and SEM. Effects of AHPS ionic monomer, contact time, dye concentration, pH, adsorbent dose, and temperature on the adsorption capacity of MB were studied. Additionally, the reusability of the composite up to five consecutive cycles was also investigated. The adsorption process was observed to obey the pseudo-second-order kinetics model, and the adsorption isotherm was best matched with the Langmuir isotherm model. Hydrogel composite (15% AHPS) achieved q_{max} of 811.5 mg/g as calculated by Langmuir equation. The calculated thermodynamic parameters ΔH, ΔG, and ΔS revealed the endothermic nature, spontaneity of the adsorption, and the positive affinity of the composites for MB adsorption with a favorable increment in the randomness at the interface between the composite and MB solution during the adsorption process.

Key words : Swelling; Hydrogel Composite; Montmorillonite; Adsorption; Methylene blue; 3-Allyloxy-2-hydroxy-1-propanesulfonic acid

1. INTRODUCTION

Dyes can be defined as complex aromatic structures which are not environmentally friendly because they are stable and more difficult to degrade in the environment[1]. Pollution of water with dyes is one of the biggest global challenges that researchers around the world are working to provide solutions. The use of dyes is widespread among many industries, as more than 10,000 dyes are applied in various industries including printing, paper, textile, and food industries [2, 3]. In spite of the industrial importance of the dyes, their discharge into the water represents a great danger to the aquatic life. It affects the life cycle of the living organisms that live in the water. Its effect may extend to cause health problems for humans, such as eye irritation and skin inflammation, and the effect may lead to cancer and causing mutations[4, 5]. Methylene blue dye (MB) is one of the common dyes in dyeing silk, cotton, and wood, but its use can cause a health effect on people such as eye burns, and on inhalation, it causes difficulty breathing, while swallowing causes nausea, vomiting, methemoglobinemia, heavy sweating, and mental confusion[5, 6]. All these implications led many researchers to develop adsorbent materials to remove the dyes from the colored wastewater. Amongst these adsorbent materials, hydrogels have achieved considerable interest in recent years as adsorbents for dyes [7-11].

Hydrogels are hydrophilic polymers but they are insoluble in water because their chains are partially cross linked, and when dipped in water or aqueous solutions they allow the water to penetrate their network structure so they

have swelling property, and they are also able to keep large amounts of water inside them relative to their mass[12, 13]. This feature (swelling property) increases the surface area of the hydrogel, which makes it a good material used to cause adsorption on its surface. Also, this feature allows enormous modifications to the hydrogel properties, amongst these modifications incorporation of inorganic materials (such as mica, kaolin, and montmorillonite) within the network structure of the hydrogels to improve their properties such as increasing their adsorption capacity, and this method has gained much attention in recent years[14-19].

Montmorillonite is one of the clay minerals composed of two tetrahedral silicate sheets and one octahedral sheet of aluminum sandwiched between the two tetrahedral sheets 2:1. It has gained interest in application as adsorbent for removing the dyes from the colored wastewater due to its cheapness, swelling property, and cation exchange capacity (CEC)[20]. The inorganic nature of the montmorillonite makes it incompatible with the polymer matrix, but this compatibility can be enhanced by entering organic molecules between the parallel layers to increase the distance between them. This organo-modification enables montmorillonite layers to be intercalated and/or exfoliated within the polymer matrices[21]. The clay minerals have been used in designing hydrogel composites as adsorbents for removing dyes from the aqueous solutions[5, 6, 22-26].According to the literature survey that we made, a study of the adsorption of the MB dye using the AAm-co-AHPS modified with organo-montmorillonite hydrogel composite was not reported, so the aim of the present study is to develop a new hydrogel composite combining between the swelling and adsorption properties of organo-montmorillonite and the ionic monomer, AHPS. The hydrogel system will provide ionic groups that contribute to the good dispersion and suspension of the montmorillonite in the adsorption solution, and also provide ionic sites that can adsorb the cationic dyes. On the other hand, the hydrogel system will facilitate the easy separation of the adsorbent material from the adsorption medium. In this report, we aim to design novel hydrogel composite by free radical polymerization and studying its swelling properties. Effect of some conditions (such as contact time, dye concentration, pH, adsorbent dose, and temperature) on the adsorption capacities of the MB has been studied.

2. EXPERIMENTAL PROCEDURE

2.1 Materials

Sodium modified montmorillonite (Na-MMT) with 0.5–5 wt% aminopropyltriethoxysilane and 15–35 wt% octadecylamine was delivered from Sigma-Aldrich Company Ltd (USA), AHPS and AAm were brought from Sigma-Aldrich Company Ltd (Germany), Methylenebisacrylamide (MBA) and Ammonium per sulfate (APS) were received from Merck (Germany), and the cationic methylene blue dye (MB) used in the adsorption studies was provided by Fluka (Switzerland).There is no further purification was done for the materials and used as received.

2.2 Characterization

FTIR spectrometer (model Cary 630) made by Agilent technologies Company was used to denote the functional groups of the prepared composites under operating conditions of the sample scan 32, resolution 8 cm^{-1}, and spectral range (wave numbers cm^{-1}) from 4000 cm^{-1} to 400 cm^{-1}. X-Ray Diffraction (XRD) (PAN analytical equipment model X Pert PRO) with a Secondary Monochromator and Cu-Ka radiation (λ=1.542Å) was used to investigate the hydrogel composites under operating conditions of the accelerating voltage 45 kV, current 35 mA, the scanning speed 0.02°/sec, and diffraction angle region (2θ) from 2° to 30°.Scanning electron microscope (SEM) (Model Quanta 250 FEG) attached with EDX Unit (Energy Dispersive X-ray Analyses) was employed to investigate the morphological structures of the hydrogel composites under operating conditions of accelerating voltage 30 K.V, resolution for Gun.1nm, and magnification 500X and 2000X. Simultaneous the rmogravimetric analyzer (Linseis STA

PT1600 TGA) was used to investigate the thermal behavior of the hydrogel composites under operating conditions of heating range 25-750 °C, heating rate of 10 °C/min, and nitrogen atmosphere.

2.3 Preparation of the hydrogel composites (HC)

All the hydrogel composites were prepared by the in-situ free radical co-polymerization method. Each hydrogel composite sample was prepared as follows: A 0.02 g of Na-MMT was added in distilled water (20 mL), then allowed to agitate for 24 h.A mixture of pre-weighed monomers (AAm & AHPS) (0.03 moles) was added to the MMT dispersion in addition to 3×10^{-4} mole of APS and MBA each. Then, the mixture was heated at 80 °C and kept under well stirring pending the gel was being formed. Five hydrogel composites (HC) was prepared by the method mentioned above at molar ratios of AHPS from 0 to 20% and the obtained composites were coded here as HC0, HC5, HC10, HC15, and HC20, respectively. The obtained composites were washed with water to remove unpolymerized monomers and uncross-linked polymers, then dried and stored.

2.4 Gel Fraction

The dried and pre-weighted hydrogel composites were dipped in distilled water for 24 h at 25°C to measure its insoluble part, and this was performed at dilute concentrations to ensure full dispersion of the hydrogel material. Then the swollen samples were removed from the water and dried at 60 °C to constant weight. The insoluble fraction in the samples was measured gravimetrically from equation 1

$$\text{Gel fraction (GF)} = \frac{\text{Dried insoluble gel}}{\text{Initial weight of gel}} \quad (1)$$

2.5 Swelling measurement

Dried and pre-weighted gel composite sample (0.05±0.001 g) contained in a nylon screen tea bag was dipped fully in plenty of distilled water (250 ml) and let to absorb the water at room temperature. Then, the samples are accurately weighed at the time (t) and return it to the water. Hydrogel composites swelling was followed periodically by extract the gel bag from the water, fast-drying, and re-weighing. Equations 2 and 3 were employed to compute the swelling ratio (SR)and equilibrium water content (EWC), respectively.

$$SR - (W_t - W_i) / W_i \quad (2)$$

$$EWC = (W_{eq} - W_i) / W_{eq} \quad (3)$$

Where W_t and W_{eq} is the weight of the dipped gel sample at time t and at equilibrium. W_i is the initial weight of the gel.

2.6 Adsorption study of MB

0.01 g of dried hydrogel composite sample was transferred into a caped tube containing distilled water, the gel composites were swelled for 24 hours until equilibrium, then the swollen sample was dipped in 20 ml dye solution at room temperature. Effect of AHPS monomer concentration, contact time, initial dye concentration, dye solution pH, gel dose, and dye solution temperature on the adsorption capacity of the hydrogel composites was studied and the amount of dye adsorption per gram at time t (q_t) and at equilibrium (q_e) was computed from equations 4 and 5, respectively. The removal percentage (*R %*) was calculated from equation 6.

$$q_t = \frac{(C^0 - C_t)V}{m} \quad (4)$$

$$q_e = \frac{(C^0 - C_e)V}{m} \quad (5)$$

$$R\,\% = \frac{(C_o - C_t)}{C_o} \times 100 \quad (6)$$

Where C_0, C_t, and C_e are the concentrations of dye solution at time = 0, time = t, and equilibrium, respectively. V(L) is the volume of dye solution, and m(g) is the mass of the pre-weighed dry hydrogel.

3. RESULTS AND DISCUSSION

3.1. Characterization of the copolymer hydrogels

Fig. 1A displays FTIR spectra of the organo-montmorillonite and the hydrogel composites (HC0, HC5, HC10, HC15, and HC20), and as shown FTIR spectrum of the organo-MMT displays a split band at 2851 and 2925 cm^{-1}whichassigned to the C–H of octadecylamine, symmetric and asymmetric stretching vibrations, respectively, the band at 1466$cm^{-1}$is ascribed to the ammonium salt[21],the band at 3645 cm^{-1} is ascribed to –OH stretching in the clay structure,1613 cm^{-1} is bending vibration of H_2O, 1095 and 995 cm^{-1} are stretching vibration of the bond between silicon and oxygen, as well as 913and 842$cm^{-1}$are ascribed to bond between multivalent metal and oxygen [27].Regarding the FTIR spectra of the hydrogel composites, the broadband observed at regions of 3100 to 3500$cm^{-1}$is belongs to the stretching vibration of N-H in the amide group, the bands observed at around1640cm^{-1}arerelated to the stretching vibration of C=O group, the band at 2929 cm^{-1} is assigned to the $-CH_2-$ stretching arising due to polymerization, and the band at 1440cm^{-1}refers to the stretching vibration of C–N group[8]. The verification of existing the anionic AHPS in the composite is the appearance of the distinctive bands at 1185 $cm^{-1}$and 1036 cm^{-1}which approved the symmetrical and asymmetrical stretching vibration of SO_2, respectively.

The hydrogel composites were subjected to thermal gravimetric analysis (TGA) to study their thermal stability, and as shown in Fig.1B.whish presents the TGA and DTG curves for the samples HC0 and HC15,it can be seen that the two composites show similar degradation characteristics and weight loss % occurred at two distinct degradation stages, the first stage ranged between 100 °C and 280 °C, and this stage displays 6.25% and 6.07% weight loss for HC0 and HC15, respectively, and this may be belonging to the releasing of moisture and bonded water. The second stage of weight loss started at about 270°C and continued up to 496 °C for HC0 and 486 °C for HC15, this step was owing to the degradation of the hydrogel polymer and breaking the carbon-carbon bonds (about 76.12% and 78.6 % weight loss for HC0 and HC15, respectively). The two degradation stages were in harmony with the main peaks of the DTG curves. The T_{max}(the temperature at the maximum degradation rate) for HC0 was 443 °C but HC15 was 438 °C and the residue %was 14.6 % and 11.5 % for HC0 and HC15. This slight difference in the thermal stability could be due to the increase in degradation rate by adding the AHPS monomer in the hydrogel chains as a result of cleavage of sulphonate groups.

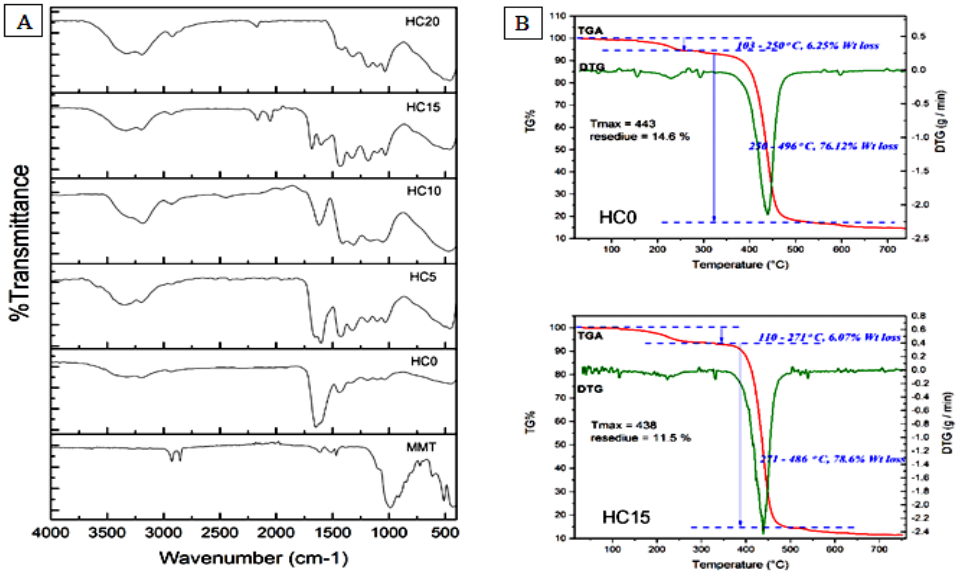

Fig. 1.FTIR spectra of organo-montmorillonite and the hydrogel composites (A), and TGA & DTG analysis of the hydrogel composite with 0%AHPS (HC0) and 15%AHPS (HC15) (B)

Fig. 2 shows the XRD patterns of organo-MMT, HC0,and HC15. A diffraction pattern of organic montmorillonite Fig.2(a)shows a strong peak corresponding to a basal spacing of 21.46 A° at the angel (2θ = 4.1), the XRD of the hydrogel composites shown in Fig. 2(b&c) indicates that the diffraction peak of MMT is disappeared in both samples. This result suggests that the MMT minerals are intercalated and completely exfoliated in the hydrogel chains matrix causing destroying the ordered structure of MMT and disappearing the d-spacing in the direction of (001) which appeared clearly in Fig. 2(a)[28].

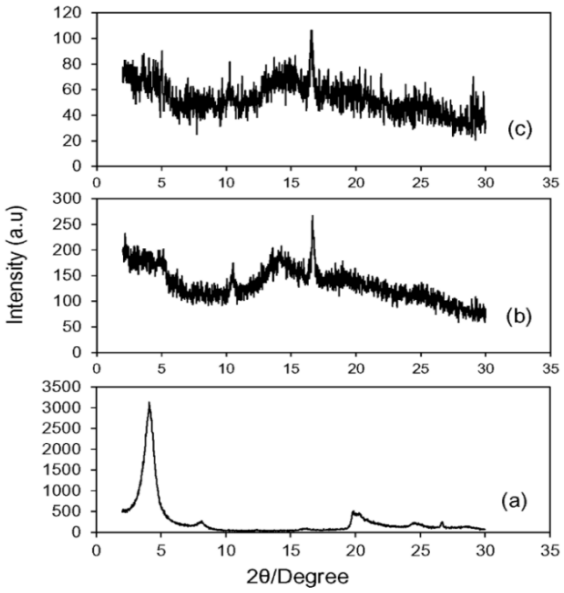

Fig. 2. XRD patterns of (a) organo-MMT, (b)hydrogel composite with 0%AHPS (HC0), and (c)hydrogel composite with 15%AHPS (HC15).

The SEM images of the hydrogel composite with 0% AHPS (HC0) and the hydrogel composite with 15% AHPS (HC15) at magnifications 500 and 2000X were presented in Fig. 3. It is obvious that the morphological structure of both hydrogel composites is porous, so they showed good performance in MB adsorption because the porous structure allows penetration of MB from dye solution onto these gel pores. There was a significant difference in the porous density and the diameter of pores between both hydrogel composites, the composite HC15 was highly porous and the average diameter of pores was 35.07 µm higher than that of HC0 which was 23.83 µm. This variance in diameter is responsible for the wide difference between the two composites in the swelling and the adsorption capacity.

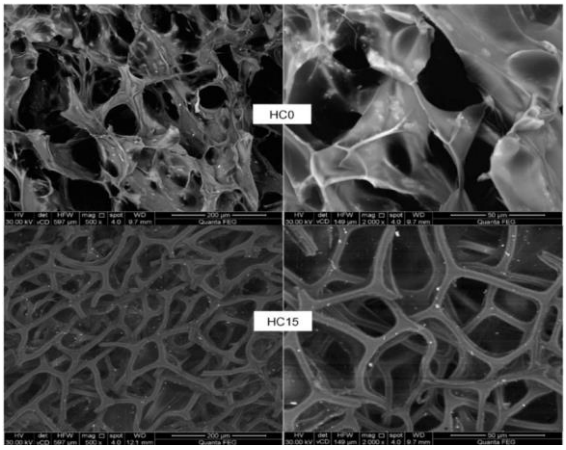

Fig. 3.SEM images of hydrogel composite with 0%AHPS(HC0), and hydrogel composite with 15%AHPS (HC15) at magnification of 500X and 2000X

3.2 Gel Fraction

Fig. 4A shows the gel fraction for the prepared hydrogel composites. It can be observed that the increase in the molar ratio of AHPS from 0% to 20% in the hydrogel composite causes a decrease in the gel fraction % from 99.1% to 72.1%. This behavior could be due to that the increasing of anionic AHPS in the feed composition results in an increase in the repulsion between the growing radical chains and hence retard the crosslinking reaction. So, the fraction of the insoluble part is dramatically reduced.

3.3 Swelling studies

Swelling capacities of the hydrogel composites at different times were studied in the distilled water at room temperature and pH=7. As indicated in Fig.4B the rate of hydrogel swelling increases over time, reaching an equilibrium point, and this point is referred to as equilibrium swelling. This usually occurs because the pores, in the beginning, are voracious to absorb water, then after that the tendency of the pores to absorb water decreases until reaching an equilibrium state at which the rate of water absorption is equal to the rate of water leakage from the pores. The craving of water absorption can be attributed to the ionic

nature of the prepared hydrogel composites, which is due to the presence of ionic sulfonate groups, and the presence of a water-loving MMT, which acts as pervading channels that allow the water molecules to easily diffuse into the hydrogel network[29]. Additionally, due to the ability of MMT molecules to ionize, the osmotic pressure increases between the hydrogel chains and the swelling medium, causing the hydrogel to crave water absorption [30]. Also, Fig.4B revealed that there was a gradual increase in the swelling capacity by increasing the percentage of AHPS in the hydrogel composite until reaching a concentration of 15%, after this concentration the capacity of the swelling decreases, and this can be ascribed to the gradually increasing of percentage of AHPS monomer from 5% to 15% causes increasing the ionic property of the gel, and hence increasing the water absorbency. After a concentration of 15%, there is a shrinkage occurs in the gel because the increase in the formation of hydrogen bonding in the gel inducing formation of aggregates in which the counter-ions condense and a drop in the osmotic pressure occurs, and this leads to a decrease in the swelling ratio.

Also, Table 1 presents the values of EWC computed quantitively by equation 3. The EWC of the hydrogel composite with 0% AHPS was 0.9507, and this value increased to0.9681-0.9803 after incorporation of AHPS into the composite system. This is due to the hydrophilicity of the AHPS monomer and modified montmorillonite.

To get more information about the mechanism of swelling of the hydrogel composites, experimental swelling kinetic data were assessed using the second-order swelling kinetic model(equation7)

$$\frac{t}{S_t} = \frac{1}{K_s S_e^2} + \frac{t}{S_e} \qquad (7)$$

Where S_t is the swelling(g/g) at time t, S_e and k_s(min^{-1}) are the theoretical equilibrium swelling capacity and the rate of swelling constant for the pseudo-second-order model, respectively. The plot of t/S_t versus t gives straight lines, S_e and k_s were computed from the slope and intercept of the plotted straight lines, respectively.

Fig.4C displays the swelling kinetics curves for the hydrogel composites and the different kinetic parameters were collected and tabulated in the Table 1.The plots gave straight

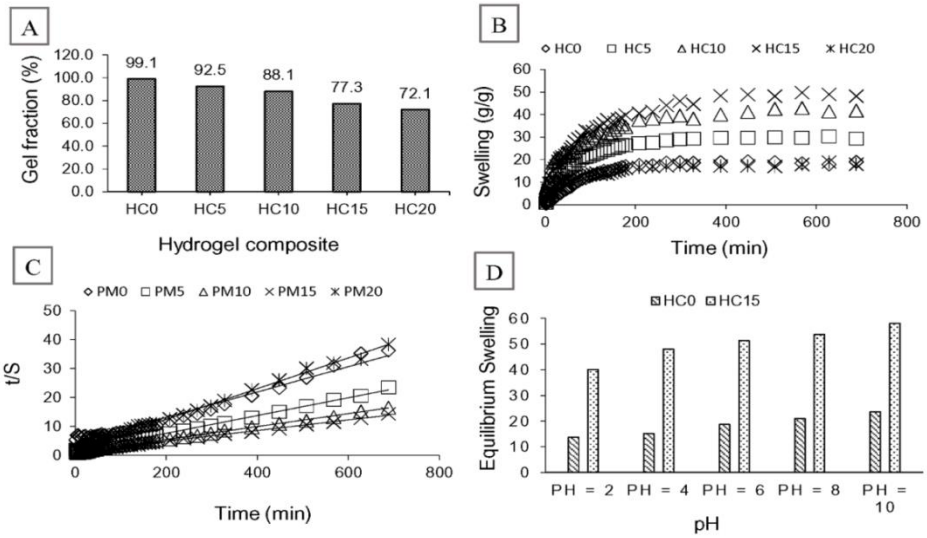

Fig. 4. Gel fraction of the prepared hydrogel composite (A), swelling capacities (B), swelling kinetics of the prepared hydrogel composites (C), and (D) effect of pH on the equilibrium swelling of the hydrogel composite without AHPS (HC0) and with 15% AHPS (HC15)

lines with good linear correlation coefficients

ranging from 0.9716 to 0.9982, and the theoretical equilibrium swelling capacity (S_e) for HC0, HC5, HC10, HC15, and HC20 were 22.85, 32.5, 44.75, 54.50, and 18.85 g/g, respectively, which were in agreement with the experimental values, Table 1. This confirms that the swelling process obeys the pseudo second-order kinetic model. Also, as shown in Table 1, the initial swelling rate for the composites with AHPS was higher than the composite without AHPS indicating the influence of the ionic nature of AHPS on the swelling rate.

Table 1. Swelling equilibrium values, swelling kinetic parameters, and equilibrium water content of the hydrogels

Hydrogel composite	S_{eq} *(g/g)* (Experimental)	EWC	S_{eq} *(g/g)* (Theoretical)	$K_s \times 10^4$ (g g^{-1} min^{-1})	K_i (g g^{-1} min^{-1})	R^2
HC0	19.28	0.9507	22.85	4.38	0.23	0.9716
HC5	30.37	0.9681	32.5	6.55	0.69	0.9982
HC10	42.90	0.9772	44.75	4.98	1	0.9955
HC15	49.71	0.9803	54.5	2.73	0.81	0.9916
HC20	18.86	0.9497	18.85	15.51	0.55	0.9959

3.4. Equilibrium swelling ratio at various pH

The swelling to equilibrium for the hydrogel composite without AHPS (HC0) and with 15 % AHPS (HC15) at various pH values 2-10 was studied at room temperature and the medium pH was adjusted using a diluted HCl solution (0.1 M) for acidic medium and NaOH solution (0.1 M) for basic medium and the results were shown in Fig. 4D.The pH of the swelling medium influenced the equilibrium swelling of both hydrogel composites as observed. The ionization of AHPS is quite and independent of pH of the medium. However, the hydrogen bonds formed between neighboring groups (such as the nitrogen atom of the amino group of the acrylamide unit, carbonyl of the amide group, and the hydrogen atom of the hydroxyl group of the AHPS unit) can form a cage-like structure. This cage-like structure has a relatively larger volume, which allows more water to be absorbed and thus increases swelling. In the acidic medium, the protonation occurs in the amino groups, so their participation in the formation of the hydrogen bonds responsible for the formation of the cage-like structure decreases, which leads to the contraction of the hydrogel and this leads to a decrease in swelling at equilibrium. In the basic medium, the amino group is deprotonated and more ready to participate in the formation of the hydrogen bonds needed to form the cage-like structure that allows large amounts of water to enter the hydrogel and the equilibrium swelling increases. Increased swelling after the AHPS enters the AAm composite is an expected action due to its ionic nature.

3.5Adsorption of MB dye

3.5.1 Effect of the ionic monomer

The impact of the ionic AHPS monomer on the hydrogel composite to adsorb the MB from the aqueous solution was examined by dipping the pre-swollen composites in neutral MB solution (100 ppm) for 24 hours contact at 25 °C and composite dose = 500 ppm, and the findings were presented in Fig. 5A. It was observed that the equilibrium adsorption capacity (q_e) increased from 116 mg/g to 198 mg/g with the increasing of AHPS ratio in the hydrogel composite from 0% to 15%, but after the concentration raised to 20% in the composite HC20 the value of q_e decreased to be 148 mg/g. This can be explained as follows: when AHPS units enter to the hydrogel composite, the number of the anionic groups in the composite increase through which the positive MB molecules can bind with, therefor the adsorption occurs. At AHPS concentration higher than 15%, the swelling of the composite

decreases as described in the swelling behavior, there for the adsorption capacity decreases.

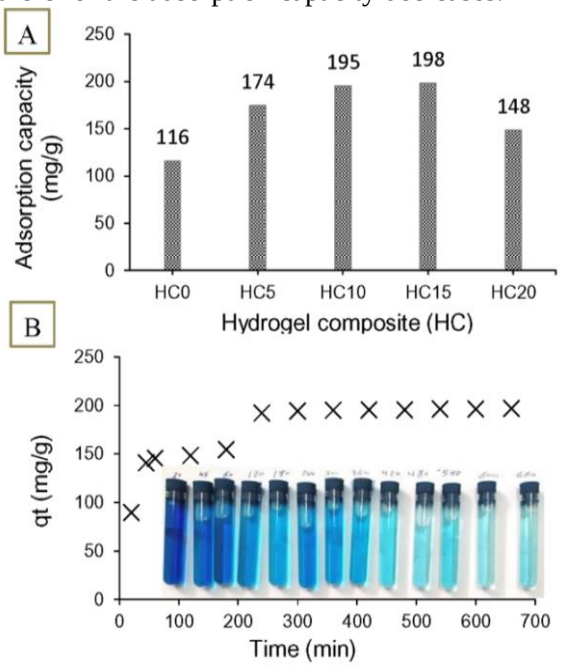

Fig. 5. Effect of (A) ionic monomer and (B) contact time on the capacity of the hydrogel composite to adsorb MB.

3.5.2 Effect of contact time

Time is very important factor for adsorption of the dye, so we studied the impact of contact time on the capacity of the hydrogel composite with 15%(HC15) to adsorb MB dye from aqueous solution at 25°C, neutral medium,$[MB]_i$=100 ppm, and [Composite dose]$_i$ = 500 ppm, and the findings were presented in Fig. 5B. As shown, the adsorption rate was rapid in the early stage of adsorption then decreased by time, until the hydrogel reached equilibrium. The initial increase in MB adsorption might be ascribed to the many available vacant sites on the hydrogel composite which bind with MB units without any hindrance and by the time more sites in the hydrogel were filled, and the adsorbed MB units make hindrance, so it was difficult for more dye molecules to reach the remaining vacant sites, and at this point, a state of equilibrium onto the hydrogel composite comes. The adsorption capacity of HC15 was 196 mg/g after 480 min contact and no significant increase after this time, so we considered 480 min to be the optimal contact time to attain the equilibrium.

3.5.3 Adsorption kinetics

To determine the MB adsorption mechanism by the hydrogel composite with 15% AHPS, the pseudo-first-order and pseudo-second-order kinetic models equations [31, 32] were used.

$$\text{Log}\,(q_e - q_t) = \log q_{e1}\,\frac{K_1 t}{2.303} \qquad (8)$$

$$\frac{t}{qt} = \frac{1}{K_2 q_{e2}^2} + \frac{t}{q_{e2}} \qquad (9)$$

Where q_t and q_e are the amount of MB dye adsorbed (mg/g) at time t and equilibrium time, respectively, $q_{e1}$and q_{e2} are the theoretical equilibrium adsorption, and k_1(min^{-1}) and k_2 (g mg^{-1} min^{-1}) are rate constants for the pseudo-first model and the pseudo-second-order model, respectively.

The findings of adsorption kinetics of the HC15 hydrogel were plotted in Fig6and data was tabulated in Table 2, and as observed the correlation coefficients (R^2) obtained from the pseudo-first-order model (R^2 = 0.9284) is lower than that of the pseudo-second-order model (R^2 = 0.997), and the difference between the experimental q_e values and the q_e values computed from the second-order kinetic model was low, while the difference was high for the first-order kinetic model, which indicates a better fit of adsorption data to the pseudo-second-order model.

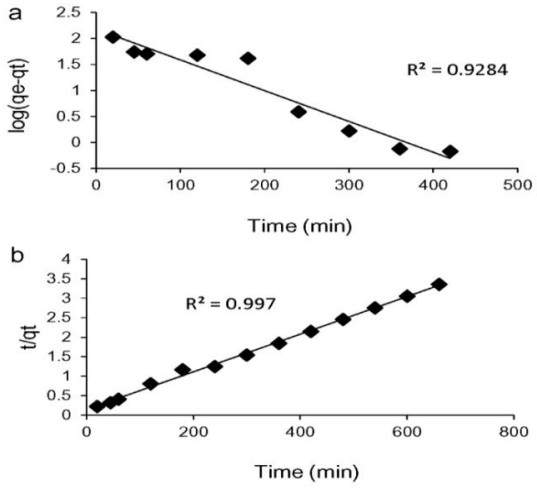

Fig. 6. Pseudo-first-order (a) and pseudo-second-order (b) kinetic models for MB adsorption kinetic data

Table 2. kinetic constants values of the MB adsorption.

$q_{e,exp}$ (mg/g)	Pseudo-first-order kinetic model			Pseudo-second-order kinetic model		
	q_{e1} (mg/g)	k_1 (min^{-1})	R^2	q_{e2} (mg/g)	K_2 (g mg^{-1} min^{-1})	R^2
196	150.65	0.0136	0.9284	207.10	0.00016	0.9970

3.5.4. Effect of initial dye concentration

The effect of the initial MB concentration on the adsorption capacity was carried out at various concentrations of MB (100–1000 ppm) while keeping all other adsorption conditions constant(pH=7, room temperature, gel dose =500 ppm, and contact time = 480 min), and the adsorption findings are given in Fig.7 (a) which shows a reduction in the adsorption capacity of the composite at low MB concentration which was due to the unsaturation of the adsorption sites. The adsorption capacity raised with the increment of the MB concentration and reached to equilibrium value at 768 mg/g at initial MB concentration 800 mg/L, and this is a result of the electrostatic repulsion between positively MB molecules which causes rapid diffusion toward the adsorption sites of the composite.

3.5.5. Adsorption isotherms

The adsorption isotherm data were analyzed using the linear forms of Langmuir[33] and Freundlich [34]isotherm models, and the findings were plotted in Fig. 7 b and c and tabulated in Table 3.

Langmuir Isotherm (equation 10)

$$\frac{C_e}{q_e} = \frac{1}{K_L q_{max}} + \frac{C_e}{q_{max}} \quad (10)$$

Where C_e(mg/l), q_e(mg/g)and q_{max}(mg/g) arethe concentration of dye at equilibrium, the quantity of dyes adsorbed at equilibrium, and the maximum adsorption capacity of the adsorbent, respectively. K_L(L/mg) is the Langmuir isotherm constant, K_L and q_{max} were obtained from the intercept and slope of plotting C_e/q_e versus C_e, respectively.

Freundlich Isotherm (equation 11)

$$\log(q_e) = \log(K_f) + \frac{1}{n}\log(C_e) \quad (11)$$

Where K_f (mg/g) and n (intensity of adsorption) are the Freundlich constants which can be computed from the intercept and slope of plotting log(q_e) versus log (C_e), respectively.

Data in Table 3 appeared that the correlation coefficient R^2 value of Freundlich isotherm model is lower than that of Langmuir isotherm, and this indicates that the Langmuir model is the best-fit model for the adsorption of MB dye onto the hydrogel composite.

Table 3. Isotherm constants for MB adsorption, ($q_{e,exp}$196 mg/g).

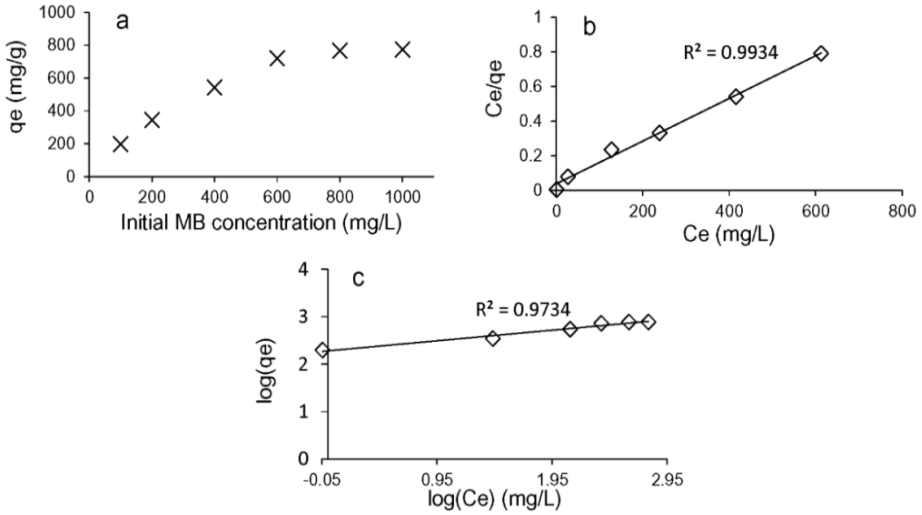

Fig. 7. Plot of (a) adsorption capacity versus initial MB concentration, (b) Langmuir isotherm model, and (c) Freundlich isotherm model.

Isotherm model	Isotherm model constant	
Langmuir	K_L (L/mg)	0.03244
	q_{max} (mg/g)	811.512
	R^2	0.9934
Freundlich	K_f (mg/g)	191.188
	n	4.485
	R^2	0.9734

3.5.6Effect of pH on MB adsorption

Here, the effect of pH range (2-10) on the adsorption of MB by the hydrogel composite was examined at room temperature, gel dose = 500 ppm, initial MB concentration = 800 ppm, and contact time = 480 min, and the findings were displayed in Fig. 8A.As seen in this figure, the adsorption capacity was low in the acidic medium and high in the basic medium, and this is expected because the competition between the hydrogen ions and the cationic MB molecules in acidic medium, on the other hand, the reduced swelling of the hydrogel composite in the acidic medium.

3.5.6 Effect of the adsorbent dosage

The effect of the adsorbent material was studied where different concentrations were used (0.5-10 g/L) while maintaining all other adsorption conditions constant (neutral MB solution, initial MB concentration = 800 mg/L, and contact time = 480 min). Figure 8B shows the results obtained using the hydrogel composite with 15%. It was observed that the removal % increased from 48% to 96% as the concentration of the adsorbent material increased from 0.5 g/L to 5 g/L, indicating a rapid increment in the removal % at this stage with an increment in the dose of the adsorbent material. This can attributed to the increment in the surface area and the availability of effective adsorption sites, which leads to an increment in the removal ratio. It was also noted that the increment in the removal ratio is slow, as it increased from 96% to 99% by increasing the adsorbent dose from 5 g/L to 7 g/L. However, after the dose 7 g/L there was no change in the ratio of removal and this may be by reason of the overlapping of the active sites at a higher dose and consequently, there was no noticeable increment in the effective surface area of adsorption. However, we noted that the removal % increased to twice after increasing the dose of the absorbent material 10 times, so we preferred that the subsequent experiments continue at 0.5 g/L.

3.5.7 Effect of temperature on dye adsorption

The effect of temperature on the removal of the dye was studied, whereby the adsorption process was carried out at three different temperatures (20, 40, and 60 °C) while maintaining all other adsorption conditions constant (neutral MB solution, initial MB concentration = 800 mg/L, adsorbent dose = 500 mg/L, and contact time = 480 min). Figure 8C shows the results we obtained when using the hydrogel composite to remove the dye. It was found that the adsorption capacity increased significantly from 872 to 1025 mg/g as the temperature increased from 20 °C to 60 °C and this indicates that the adsorption process is preferred at elevated temperatures. This increase is due to the following reason: When the temperature is raised, the hydrogel composite network is swollen, so the surface area exposed to the adsorption increases, and there are a greater number of active sites that are associated with the dye molecules in the adsorption process. On the other hand, when the temperature increases, the viscosity of the dye solution decreases, and the rate of diffusion of the dye particles increases, allowing a greater number of dye molecules to penetrate the hydrogel network and bind to the active sites. From the above, it is clear that the adsorption process of MB dye on the surface of the hydrogel composite with 15%AHPS is a heat-absorbing process (endothermic).

To confirm this result, the thermodynamic parameters such as Gibbs free energy change ΔG (KJ mol^{-1}), standard enthalpy change ΔH(KJ mol^{-1}), and standard entropy change ΔS($JK^{-1}mol^{-1}$), (Equations 12-14) were also studied.

$$\ln k_c = \frac{\Delta S}{R} - \frac{\Delta H}{RT} \quad (12)$$

$$K_c = {C_{Ae}}/{C_e} \quad (13)$$

$$\Delta G = -RT\,ln\,k_c \quad (14)$$

Where K_C, C_{Ae}, and C_e are the equilibrium constant, the amount of dye adsorbed (mg/g) at equilibrium, and the equilibrium concentration (mg L^{-1}) of the dye in the solution, respectively, T and R are the solution temperature (in kelvin) and the universal gas constant (0.008314K J mol^{-1} K^{-1}), respectively. ΔH and ΔS were computed from the slope and intercept of van't Hoff plots of LnK_C versus 1/T(Figure not presented).The values of ΔH, ΔS, and ΔG for MB adsorbed by the hydrogel composite are listed in Table4, and by looking at the results, we note the positive value of enthalpy change ΔH (8.0445 KJ mol^{-1}) which confirm that the adsorption of MB onto the hydrogel composite is physisorption and endothermic. The positive entropy change ΔS (0.0347 KJ K^{-1} mol^{-1}) value exhibited the randomness of MB molecules increased at the interface between the composite and MB solution during the adsorption process, but the increase in the negative values of ΔG predict the spontaneous nature of the MB adsorption and the adsorption is favorable at high temperatures.

Table 4 Thermodynamic parameters for the adsorption of MB dye into hydrogel composite

ΔH (KJ mol^{-1})	ΔS (KJ K^{-1} mol^{-1})	- ΔG (KJ mol^{-1})		
		293 K	313 K	333 K
8.0445	0.0347	2.129	2.856	3.517

3.5.8 Reusability

One of the most important parameters in the practical application of any adsorbent is its lifetime because its performance for a longer period of time leads to a significant reduction in the cost of treatment. Thus, it is worth studying the evaluation of the stability of the adsorbent material and its reuse. This study was carried out by repeating the removal of the dye five times with the same adsorbent material. After each cycle, the adsorbent material was washed with 0.1 M HCl and re-used again to remove the dye. Figure 8D shows the reusability results of the hydrogel composite with 15% AHPS. The results showed the effectiveness of the re-use of the adsorbent material to adsorb the dye where the removal ratio was after the first cycle 86.4% and after the fifth cycle 83.96% where the initial concentration of the dye 200 mg/L.

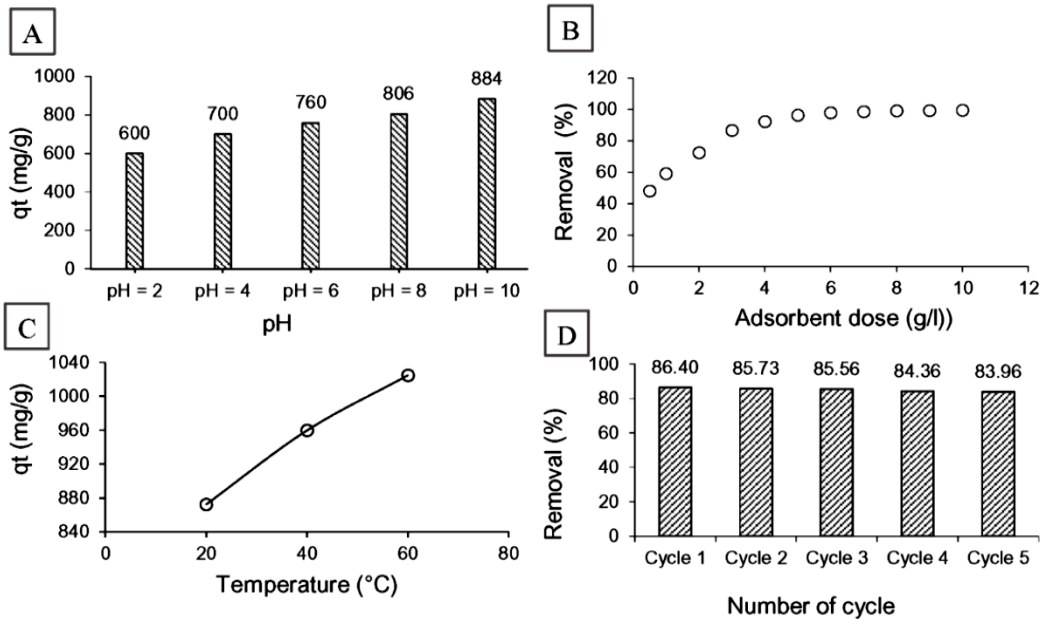

Fig. 8. Effect of pH (A), the adsorbent dose (B), and Temperature (C) on the MB adsorption by the hydrogel composite, and (D) MB adsorptioncycles of reuse of the hydrogel composite with 15 % AHPS

This slight decrease in efficiency, possibly due to the loss of the adsorbent during washing. These results give this material an application and economic advantage as an adsorbent to remove the MB dye from the colored water.

3.5.9 Comparison q_{max} with the previous studies

Given the great diversity among conditions of adsorption processes in other reported studies, it is difficult to compare the efficacy of any adsorbents with other adsorbents previously reported in the literature. However, to highlight the importance of this study and its results in adsorption of the MB dye, the comparison was facilitated by presenting the maximum adsorption values (q_{max}) calculated from the Langmuir isotherm equation obtained in previous studies in Table 5. Looking at the values presented in the table and comparing them with the value obtained in our study, it is clear that the prepared hydrogel composite can be used very effectively in adsorbing the MB dye from its aqueous solutions.

SEM, TGA, and XRD. The hydrogel composite with 15% AHPS achieved high water swelling ratio 49.71 g water/g gel and tested as adsorbent MB from aqueous solution. The adsorption experiments demonstrated the validity of the tested composite for the effective adsorption of the MB dye, where the results showed that the effectiveness of the adsorbent material was 768 mg dye/g composite where the initial concentration of the dye was 800 mg/L, and the practical results were consistent with the theoretical calculations of the Langmuir equation, which showed that the maximum adsorption capacity of the adsorbent material is 811.5 mg/g. The study of adsorption kinetics resulted in compatibility of the Pseudo-second-order kinetic model with the practical results of adsorption. Calculations of the thermodynamic parameters also contributed to understanding the nature of adsorption, as it showed that the adsorption of MB onto the hydrogel composite with 15% AHPS is physical and endothermic. And the reusability studies revealed that the obtained adsorbent material has a good activity even after five cycles of reuse.

Table 5. Comparison of the present work with previous studies.

Adsorbent	q_{max} (mg/g)	Reference
Acrylamido-2-methyl-1-propanesulfonic acid-based hydrogel	261.78	[8]
Lignocellulose-g-poly(acrylic acid)/montmorillonite	1994.38	[35]
Decanted Moroccan clay	114.16	[36]
N-tert-butylmaleamic acid-based hydrogel	384.6	[37]
Activated carbon	882.4	[38]
Straw with Fe_3O_4 magnetic nanoparticles	1374.6	[39]
Activated biochar	77.3	[40]
Xanthan gum-co-acrylic acid/graphene oxide	793.65	[41]
(AAm-co-AHPS)/ Organo-MMT	811.5	This study

CONCLUSION

In this work, novel hydrogel composite based on AAm, AHPS, and modified MMT was synthesized successfully to remove the MB dye from aqueous solution. Structure of the hydrogel composites was confirmed by FTIR,

ACKNOWLEDGEMENT

The authors would like to present words of thanks and gratitude to the Department of Chemistry, Faculty of Science, Al-Azhar

University for their continuous support and provision of all research work needs.

REFERENCES

[1] Kaşgöz, H. and A. Durmus, *Dye removal by a novel hydrogel-clay nanocomposite with enhanced swelling properties.* Polymers for Advanced Technologies, 2008. **19**(7): p. 838-845.

[2] Lee, J.W., S.P. Choi, R. Thiruvenkatachari, W.G. Shim, and H. Moon, *Evaluation of the performance of adsorption and coagulation processes for the maximum removal of reactive dyes.* Dyes and Pigments, 2006. **69**(3): p. 196-203.

[3] Hai, F.I., K. Yamamoto, and K. Fukushi, *Hybrid treatment systems for dye wastewater.* Critical Reviews in Environmental Science and Technology, 2007. **37**(4): p. 315-377.

[4] Anitha., A., S.P. Kumar, and S.K. Kumar, *Synthesis of nano-sized chitosan blended polyvinyl alcohol for the removal of Eosin Yellow dye from aqueous solution.* Journal of Water Process Engineering, 2016. **13**: p. 127-136.

[5] Wang, L., J. Zhang, and A. Wang, *Fast removal of methylene blue from aqueous solution by adsorption onto chitosan-g-poly (acrylic acid)/attapulgite composite.* Desalination, 2011. **266**(1): p. 33-39.

[6] Wang, W., Y. Zhao, H. Bai, T. Zhang, V. Ibarra-Galvan, and S. Song, *Methylene blue removal from water using the hydrogel beads of poly(vinyl alcohol)-sodium alginate-chitosan-montmorillonite.* Carbohydrate Polymers, 2018. **198**: p. 518-528.

[7] Ibrahim, A.G., F. Abdel Hai, H. Abd El-Wahab, and H. Mahmoud, *Synthesis, characterization, swelling studies and dye removal of chemically crosslinked acrylic acid/acrylamide/N, N-dimethyl acrylamide hydrogels.* American Journal of Applied Chemistry 2016. **4**(6): p. 221-234.

[8] Bera, R., A. Dey, and D. Chakrabarty, *Tuning of the swelling and dye removal efficacy of poly (acrylamide-AMPS)-based smart hydrogel.* Separation Science and Technology, 2017. **52**(4): p. 743-755.

[9] Ibrahim, A.G., F. Abdel Hai, H. Abd El-Wahab, and H. Aboelanin, *Methylene blue removal using a novel hydrogel containing 3-Allyloxy-2-hydroxy-1-propanesulfonic acid sodium salt.* Advances in Polymer Technology, 2018. **37**(8): p. 3561-3573.

[10] Hernandez-Martínez, A.R., J.A. Lujan-Montelongo, C. Silva-Cuevas, J.D. Mota-Morales, M. Cortez-Valadez, Á.D.J. Ruíz-Baltazar, M. Cruz, and J. Herrera-Ordonez, *Swelling and methylene blue adsorption of poly(N,N-dimethylacrylamide-co-2-hydroxyethyl methacrylate) hydrogel.* Reactive and Functional Polymers, 2018. **122**: p. 75-84.

[11] Ibrahim, A.G., A.Z. Sayed, H. Abd El-Wahab, and M.M. Sayah, *Synthesis of a hydrogel by grafting of acrylamide-co-sodium methacrylate onto chitosan for effective adsorption of Fuchsin basic dye.* International Journal of Biological Macromolecules, 2020. **159**: p. 422-432.

[12] Kabiri, K., H. Omidian, S.A. Hashemi, and M.J. Zohuriaan-Mehr, *Synthesis of fast-swelling superabsorbent hydrogels: Effect of crosslinker type and concentration on porosity and absorption rate.* European Polymer Journal, 2003. **39**(7): p. 1341-1348.

[13] Nagarpita, M.V., P. Roy, S.B. Shruthi, and R.R.N. Sailaja, *Synthesis and swelling characteristics of chitosan and CMC grafted sodium acrylate-co-acrylamide using modified nanoclay and examining its efficacy for removal of dyes.* International Journal of Biological Macromolecules, 2017. **102**: p. 1226-1240.

[14] Noppakundilograt, S., K. Sonjaipanich, N. Thongchul, and S. Kiatkamjornwong, *Syntheses, characterization, and antibacterial activity of chitosan grafted hydrogels and associated mica-containing nanocomposite hydrogels.* Journal of Applied Polymer Science, 2013. **127**(6): p. 4927-4938.

[15] Foungfung, D., S. Phattanarudee, N. Seetapan, and S. Kiatkamjornwong, *Acrylamide-itaconic acid superabsorbent polymers and superabsorbent polymer/mica nanocomposites.* Polymers for Advanced Technologies, 2011. **22**(5): p. 635-647.

[16] Shirsath, S.R., A.P. Patil, B.A. Bhanvase, and S.H. Sonawane, *Ultrasonically prepared poly(acrylamide)-kaolin composite hydrogel for removal of crystal violet dye from wastewater.* Journal of Environmental Chemical Engineering, 2015. **3**(2): p. 1152-1162.

[17] Hosseinzadeh, H. and M. Sadeghi, *Preparation and swelling behaviour of*

carboxymethylcellulose-g-poly(sodium acrylate) / kaolin super absorbent hydrogel composites. Asian Journal of Chemistry, 2012. **24**(1): p. 85-88.

[18] Karadağ, E., A. Nalbantoğlu, S. Kundakci, and Ö.B. Üzüm, *Highly Swollen Polymer/Clay Composite Sorbent-Based AAm/AMPS Hydrogels and Semi-IPNs Composed of Carboxymethyl Cellulose and Montmorillonite and Cross-Linked by PEGDA.* Polymer - Plastics Technology and Engineering, 2014. **53**(1): p. 54-64.

[19] Karadağ, E., B. Hasgül, S. Kundakci, and Ö.B. Üzüm, *A study of polymer/clay hybrid composite sorbent-based AAm/SMA hydrogels and semi-IPNs composed of l-carrageenan and montmorillonite for water and dye sorption.* Advances in Polymer Technology, 2014. **33**(4).

[20] He, H., L. Ma, J. Zhu, R.L. Frost, B.K.G. Theng, and F. Bergaya, *Synthesis of organoclays: A critical review and some unresolved issues.* Applied Clay Science, 2014. **100**(C): p. 22-28.

[21] Arroyo, M., M.A. López-Manchado, and B. Herrero, *Organo-montmorillonite as substitute of carbon black in natural rubber compounds.* Polymer, 2003. **44**(8): p. 2447-2453.

[22] Kundakci, S., Ö.B. Üzüm, and E. Karadağ, *Swelling and dye sorption studies of acrylamide/2-acrylamido-2-methyl-1-propanesulfonic acid/bentonite highly swollen composite hydrogels.* Reactive and functional polymers, 2008. **68**(2): p. 458-473.

[23] Kundakci, S., Ö.B. Üzüm, and E. Karadağ, *A new composite sorbent for water and dye uptake: Highly swollen acrylamide/ 2-acrylamido-2-methyl-1-propanesulfonic acid/ clay hydrogels crosslinked by 1, 4-butanediol dimethacrylate.* Polymer Composites, 2009. **30**(1): p. 29-37.

[24] Lu, Q., J. Zheng, J. Yu, S. Yang, D. Ma, W. Yang, and J. Gao, *Synthesis and Adsorption Properties for Cationic Dyes of Acrylic Acid/Vermiculite Hydrogel Initiated by Glow-Discharge-Electrolysis Plasma*. Advances in Polymer Technology, 2018. **37**(4): p. 996-1007.

[25] Hosseinzadeh, H. and N. Khoshnood, *Removal of cationic dyes by poly(AA-co-AMPS)/ montmorillonite nanocomposite hydrogel.* Desalination and Water Treatment, 2016. **57**(14): p. 6372-6383.

[26] Peighambardoust, S.J., O. Aghamohammadi-Bavil, R. Foroutan, and N. Arsalani, *Removal of malachite green using carboxymethyl cellulose-g-polyacrylamide/montmorillonite nanocomposite hydrogel.* International Journal of Biological Macromolecules, 2020. **159**: p. 1122-1131.

[27] Nakhjiri, M.T., G.B. Marandi, and M. Kurdtabar, *Effect of bis [2-(methacryloyloxy) ethyl] phosphate as a crosslinker on poly (AAm-co-AMPS)/Na-MMT hydrogel nanocomposite as potential adsorbent for dyes: kinetic, isotherm and thermodynamic study.* Journal of Polymer Research, 2018. **25**(11): p. 244.

[28] Mahdavinia, G.R., H. Aghaie, H. Sheykhloie, M.T. Vardini, and H. Etemadi, *Synthesis of CarAlg/MMt nanocomposite hydrogels and adsorption of cationic crystal violet.* Carbohydrate Polymers, 2013. **98**(1): p. 358-365.

[29] Ilgin, P., H. Durak, and A. Gür, *A Novel pH-Responsive p(AAm-co-METAC)/MMT Composite Hydrogel: Synthesis, Characterization and Its Absorption Performance on Heavy Metal İons.* Polymer - Plastics Technology and Engineering, 2015. **54**(6): p. 603-615.

[30] Olad, A., M. Pourkhiyabi, H. Gharekhani, and F. Doustdar, *Semi-IPN superabsorbent nanocomposite based on sodium alginate and montmorillonite: Reaction parameters and swelling characteristics.* Carbohydrate Polymers, 2018. **190**: p. 295-306.

[31] Yuh-Shan, H., *Citation review of Lagergren kinetic rate equation on adsorption reactions.* Scientometrics, 2004. **59**(1): p. 171-177.

[32] Ho, Y.-S., *Pseudo-isotherms using a second order kinetic expression constant.* Adsorption, 2004. **10**(2): p. 151-158.

[33] Greluk, M. and Z. Hubicki, *Kinetics, isotherm and thermodynamic studies of Reactive Black 5 removal by acid acrylic resins.* Chemical Engineering Journal, 2010. **162**(3): p. 919-926.

[34] Monier, M. and D.A. Abdel-Latif, *Preparation of cross-linked magnetic chitosan-phenylthiourea resin for adsorption of Hg(II), Cd(II) and Zn(II) ions from aqueous solutions.* Journal of Hazardous Materials, 2012. **209-210**: p. 240-249.

[35] Shi, Y., Z. Xue, X. Wang, L. Wang, and A. Wang, *Removal of methylene blue from aqueous solution by sorption on lignocellulose-*

g-poly(acrylic acid)/montmorillonite three-dimensional cross-linked polymeric network hydrogels. Polymer Bulletin, 2013. **70**(4): p. 1163-1179.

[36] Elmoubarki, R., F.Z. Mahjoubi, H. Tounsadi, J. Moustadraf, M. Abdennouri, A. Zouhri, A. El Albani, and N. Barka, *Adsorption of textile dyes on raw and decanted Moroccan clays: Kinetics, equilibrium and thermodynamics.* Water Resources and Industry, 2015. **9**: p. 16-29.

[37] Ilgin, P., H. Ozay, and O. Ozay, *Selective adsorption of cationic dyes from colored noxious effluent using a novel N-tert-butylmaleamic acid based hydrogels.* Reactive and Functional Polymers, 2019. **142**: p. 189-198.

[38] Chang, *The Langmuir monolayer adsorption model of organic matter into effective pores in activated carbon.* Journal of Colloid and Interface Science, 2013. **389**(1): p. 213-219.

[39] Ebrahimian Pirbazari, A., E. Saberikhah, and S.S. Habibzadeh Kozani, *Fe3O4-wheat straw: Preparation, characterization and its application for methylene blue adsorption.* Water Resources and Industry, 2014. **7-8**: p. 23-37.

[40] Wang, Y., Y. Zhang, S. Li, W. Zhong, and W. Wei, *Enhanced methylene blue adsorption onto activated reed-derived biochar by tannic acid.* Journal of Molecular Liquids, 2018. **268**: p. 658-666.

[41] Makhado, E., S. Pandey, and J. Ramontja, *Microwave assisted synthesis of xanthan gum-cl-poly (acrylic acid) based-reduced graphene oxide hydrogel composite for adsorption of methylene blue and methyl violet from aqueous solution.* International Journal of Biological Macromolecules, 2018. **119**: p. 255-269.

تحضير وتوصيف متراكبات هيدروجيل (AAm-co-AHPS) / MMT
للإمتزاز الفعال لصبغة الميثيلين الأزرق من المحاليل المائية

أمين محمد القوني[1] – أحمد جلال إبراهيم[2] – ماهر حامد أبو الفرح[3] – فرج عبد الحي[4]

[1،2، 4] قسم الكيماء – كلية العلوم – جامعة الازهر – القاهرة ـ مصر

[3] المعامل المركزية للهيئة المصرية العامة للثروة المعدنية – الدقي – الجيزة ـ مصر

الملخص العربي

في هذه الدراسة تم تحضير سلسلة من متراكبات الهيدروجيل باستخدام مونومر الاكريلاميد (AAm) مع كميات مختلفة من مونومر الملح الصوديومي ل-3- اليل اوكسي -2- هيدروكسي -1- بروبان سلفونيك اسيد (AHPS) مع ادخال خام المونتموريلونيت بنسبة ثابتة لكل العينات بطريقة البلمرة بالجذور الحرة. تم دراسة قدرة عينات الهيدروجيل المحضره علي الانتفاش فى الماء و امتزاز صبغة الميثيلين الزرقاء من المحاليل المائية. كما تمت دراسة تأثير نسبة مونومر AHPS علي خواص متراكبات الهيدروجيل المحضره عند النسبالمولارية =AAm/AHPS (100/0, 95/5, 90/10, 85/15, 80/20) ووصلت اعلي نسبة انتفاش الي 49.71 g/g في العينة التي تحتوي علي 15% من مونومر AHPS. تم توصيف البوليمرات الناتجه من عملية البلمرة باستخدام مطياف الأشعة تحت الحمراء (FTIR) والميكروسكوب الالكتروني الماسح (SEM) كما تم قياس درجة الثبات الحراري باستخدام جهاز التحليل الحراري الوزني (TGA) كما تم اثبات التركيب البلوري باستخدام مقياس حيود الاشعة السينية (XRD). تم دراسة تأثير كلا من التركيز الابتدائي للصبغة وزمن التلامس والأس الهيدروجيني وتركيز الهيدروجيل (المادة الممتصة) ودرجة الحرارة علي عملية امتزاز صبغة الميثلين الزرقاء بالإضافة الي دراسة امكانية اعادة استخدام البوليمرات المحضرة ووجد ان المواد المحضرة قابلة لاعادة الاستخدام بفاعلية حتي خمس مرات. تم دراسة حركية نماذج الامتزاز ووجد ان التفاعلات بين الهيدروجل وصبغة الميثيلين الزرقاء تتبع تفاعلات الرتبة الثانية الكاذبة كما أنه بدراسة نماذج الامتزاز الايزوثرمية وجد ان عملية امتزاز صبغة الميثيلين الزرقاء علي متراكبات الهيدروجيل المحضرة تتوافق مع نموذج Langmuir حيث حققت العينة المحتوية علي 15% AHPS اقصي قيمة امتصاص q_{max} = 811.5 mg/g طبقا نموذج Langmuir. بدراسة نماذج الديناميكا الحرارية وجد ان قيم ΔH و ΔG و ΔS تدل علي ان التفاعل ماص للحرارة وتلقائي وعشوائية النظام تميل الي الزيادة عند سطح التلامس صلب/سائل اثناء عملية الامتزاز.